

AMMRC TR 83-3

Army Materials and Mechanics Res. **AD A127822**  
To  
Watertown, Massachusetts 02172

# **THE MEASUREMENT OF X-RAY RESIDUAL STRESS IN TEXTURED CUBIC MATERIALS**

**CHARLES P. GAZZARA**

**MATERIALS CHARACTERIZATION DIVISION**

**JANUARY 1983**

Approved for public release; distribution unlimited.

**ARMY MATERIALS AND MECHANICS RESEARCH CENTER**  
**Watertown, Massachusetts 02172**

The findings in this report are not to be construed as an official Department of the Army position, unless so designated by other authorized documents.

Mention of any trade names or manufacturers in this report shall not be construed as advertising nor as an official indorsement or approval of such products or companies by the United States Government.

#### DISPOSITION INSTRUCTIONS

Destroy this report when it is no longer needed.  
Do not return it to the originator.

SECURITY CLASSIFICATION OF THIS PAGE (When Data Entered)

DD FORM 1 JAN 73 1473 EDITION OF 1 NOV 65 IS OBSOLETE

SECURITY CLASSIFICATION OF THIS PAGE (When Data Entered)

Block No. 20

## ABSTRACT

An X-ray diffraction procedure for measuring residual stress assumes a linear relationship between the d spacing and  $\sin^2\psi$  in isotropic materials. This study attempts to deal with the use of such a relationship in textured steel and aluminum using parallel beam optics. It was found that a phase difference occurs in the d spacing and the X-ray intensity of the  $\text{CrK}\alpha$  diffraction peak with  $\psi$  resulting in errors in computing the residual stress. Possible contributing factors are considered, such as systematic errors, specimen preparation, absorption, grain size, and the optical system employed.

## CONTENTS

	Page
INTRODUCTION . . . . .	1
X-RAY DIFFRACTION SYSTEM . . . . .	3
MATERIALS. . . . .	4
PHASE EFFECT . . . . .	4
SYSTEMATIC ERRORS. . . . .	4
DIVERGENT BEAM GEOMETRY. . . . .	8
REPRODUCIBILITY AND CONFIDENCE . . . . .	9
ALUMINUM TEXTURED ALLOY. . . . .	9
CONCLUSIONS. . . . .	11
ACKNOWLEDGMENTS. . . . .	13
REFERENCES . . . . .	14



## INTRODUCTION

The X-ray determination of residual stresses in textured materials has been treated by many investigators. One reason for such great activity in this area is the preponderance of factors influencing the departure of textured material from the ideal isotropic behavior in that the  $d$  spacing vs.  $\sin^2\psi$  relationship is not linear but rather is oscillatory. A current synopsis of these factors is given by Dölle<sup>1</sup> and by Dölle and Cohen.<sup>2</sup>

A popular method for correcting for the effects of texture on the X-ray residual stress was developed by Marion and Cohen.<sup>3</sup> In this treatment, oscillations in  $d$  with  $\sin^2\psi$  were correlated with the deformation texture using an approach introduced by W. Weidemann<sup>4</sup> in the form:

$$d = (d_{\max} - d_B) f(\alpha, \beta) + d_B \quad (1)$$

where

$f(\alpha, \beta)$  is a distribution function of a given  $(h\ k\ l)$  plane relative to sample coordinates

$\alpha$  is the longitude on a pole figure with center at sample normal

$\beta$  is the latitude

$d_{\max}$  is the largest lattice spacing (such as in some localized region A undergoing maximum deformation due to energetically favorable orientation relative to deformation geometry)

$d_B$  is the smallest lattice spacing (such as in some localized region B undergoing least deformation).

Placing Equation (1) in a general form including the effect of residual stress,  $\sigma$  on  $d$  (Reference 3) yields:

$$d_{\phi, \psi} = (d_{\max} - d_B) f(\alpha, \beta) + d_{\perp} \frac{(1 + \nu)}{E} \sigma_{\phi} \sin^2 \psi + d_B \quad (2)$$

- 
1. DÖLLE, H. The Influence of Multiaxial Stress States, Stress Gradients and Elastic Anisotropy on the Evaluation of Residual Stresses by X-Rays. J. Appl. Cryst, v. 12, 1979, p. 489.
  2. DÖLLE, H., and COHEN, J. B. Evaluation of Residual Stresses in Textured Cubic Metals. Met. Trans. A., v. 11A, 1980, p. 831.
  3. MARION, R. H., and COHEN, J. C. Anomalies in Measurement of Residual Stress by X-Ray Diffraction. Adv. X-Ray Anal., v. 18, 1975, p. 466.
  4. WEIDEMANN, W., Phd. Thesis, Technische Hochschule. Aachen, Germany, 1966, Synopsis in Bollenroth, V. F., Hauk, V., as Zur Dentung der Gittereigenverformungen in plastisch verformtem-Eisen, Arch für Eisen, v. 10, 1967, p. 793.

where

- $\phi$  - angle around specimen normal
- $d_{\perp}$  - spacing along specimen normal
- $\nu$  - Poisson's ratio
- $E$  - modulus of elasticity.

Marion and Cohen aligned the angle  $\psi$  along the rolling direction (R.D.) of  $\alpha$ -Fe for the reflecting plane (211) with the highest diffracting Bragg angle,  $2\theta$ , using  $\text{CrK}\alpha$  X-radiation. For this technique, the elastic constants are assumed to be isotropic and applicable to the X-ray case. As may be deduced from Equations (1) and (2) the oscillations in  $d$  are in phase with the distribution function  $f(\alpha, \beta)$ , i.e., the diffracted peak-intensity maxima intensity should align with the  $d$  maxima.

The oscillations along R.D. of  $d$  vs.  $\sin^2\psi$  were treated by Shiraiwa and Sakamoto<sup>5</sup> to determine the effect of elastic constants and plastic anisotropy in textured cold-rolled steel specimens. The elastic constants employed were taken from single crystal data. The  $\alpha=0$  line through the {211} pole figure revealed  $f(0, \psi)$  maxima at  $\psi=0^\circ$  and  $60^\circ$  contributed by the (211)  $[01\bar{1}]$  component of texture, at  $\psi=19.5^\circ$  from the (111)  $[21\bar{1}]$  texture component, and at  $\psi=35.3^\circ$  from the (100)  $[01\bar{1}]$  texture component.

A generalized treatment was developed by Dölle and Hauk<sup>6</sup> for relating the lattice strain to the elastic constants, and the angles  $\phi$  and  $\psi$ , for anisotropic materials. For the (211) reflection, oscillations also exist parallel to R.D. in  $(d_{0,\psi} - d_0)/d_0$  vs.  $\sin^2\psi$ . For this particular plot, however, Hauk and Sesemann<sup>7</sup> found that two texture-dependent directions occur in which the lattice strain is isotropic. This procedure by itself, although implicitly correct, may be of questionable accuracy in yielding limited data at low  $\psi$  values.

In addition to the previously cited factors, oscillations may also be present due to grain coupling, micro-stress inhomogeneities, and shear-stress and large-stress gradients. In the case of sharp-stress gradients (Peiter and Lode, as discussed in Reference 1) the nonlinearity of  $d$  with  $\sin^2\psi$  is smaller than the previously discussed effects. In addition, this effect can be isolated with surface removal, i.e., by applying an electropolishing procedure.

Oscillations are also likely to occur if the grain size is too large. Although the likelihood of such phenomena taking place is greatest in a recrystallized material, the possibility exists that deformed alloys might exhibit such oscillations. Fortunately, these grain size oscillations may be simply detected by repeating the measurements after translational relocation of the specimen, which has the effect of altering the magnitude and location of the oscillations.<sup>2</sup>

- 
5. SHIRAIWA, T., and SAKAMOTO, Y. The X-Ray Stress Measurement of the Deformed Steel Having Preferred Orientation, Soc. Mat. Sci., 1970, Kyoto, Japan, p. 25.
  6. DÖLLE, H., and HAUK, V. Einfluss der Mechanischen Anisotropie de Vielkristalls (Textur) auf die Röntgenographische Spannungermittlung, v. 69, 1978, p. 410.
  7. HAUK, V., and SESEMANN, H. Abweichungen von Linearen Gitterbenenabstandsverteilungen in Kubischen Metallen und ihre Berücksichtigung bei der Röntgenographischen Spannungermittlung, v. 67, 1976, p. 646.



In order to avoid these problems associated with textured materials, Dölle and Cohen<sup>2</sup> suggest employing {h00} and {hhh} reflections, which retain the linear  $d$  vs.  $\sin^2\psi$  character. As an alternative, the {310} reflection is recommended in place of the {211} in steel to avoid these texture effects along the R.D.

In this study, an apparent phase difference between  $d$  and  $f(0,\psi)$  along the R.D. in textured material is discussed. This phase difference is significant when correction procedures for oscillations along the R.D. are employed, i.e., the Marion-Cohen method.

## X-RAY DIFFRACTION SYSTEM

For the most part, the X-ray diffraction data presented in this report was taken with a Rigaku Strainflex MSF/PSF system. A chromium (Cr) X-ray tube operated at 30 kV and 10 mA was the source of the  $K\alpha$  filtered radiation utilized in this work. A standard  $1^\circ$  divergence beam and receiving slit with a built in collimator provided the specified "parallel beam" optics.

The X-ray geometry illustrating the optical variables is shown in Figure 1.  $N_s$  is the specimen normal, whereas the diffraction system normal is  $N_R$ . The angular displacement between  $N_s$  and  $N_R$  is denoted by  $\delta$ , and is ideally equal to 0.  $\psi_0$  is the inclination angle built into the Rigaku Strainflex, whereas  $\psi$  is the corrected angle. During an X-ray "2 $\theta$  scan", the Rigaku X-ray  $\psi$  is generally used in X-ray residual stress calculations. The angle  $\eta$  is defined as  $90-\theta$ .

The position of the diffraction peak maximum was obtained from the recorder chart diffractogram employing the side slope method. It was found that the parabolic fitting method and the midpoint method (when sufficient background data were recorded) consistently gave similar results, but that the side slope method was more convenient to work with.

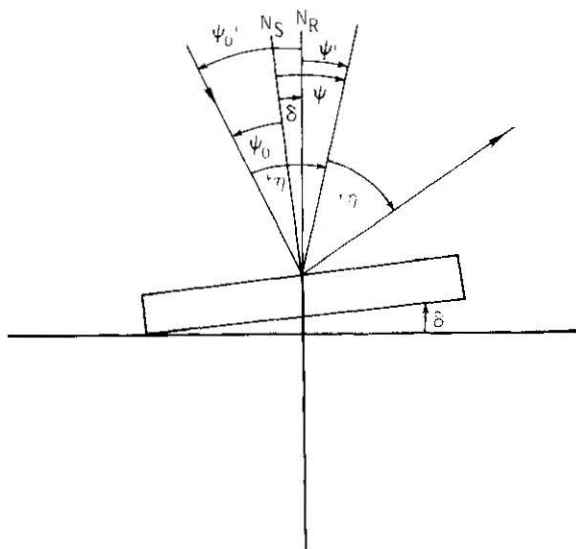


Figure 1. Schematic drawing of X-ray diffraction geometry for the Rigaku Strainflex system.

## MATERIALS

The three textured specimens considered in this study are a martensitic steel, a cold-rolled iron (Fe), and an Al alloy.

### a. Martensitic steel\*

Specimen 1 was cut from a 4340 steel plate that had been austenitized at 1550°F, rolled to a reduction of 90% over a declining temperature range and, finally, water-quenched from the "bay" region. This specimen revealed a high degree of texture.

### b. Pure iron

Specimen CR1 was fabricated by (1) arc melting electrolytic iron, (2) normalizing at 940°C for 20 min in air and air cooling, (3) machining to a thickness of 0.140", (4) cross rolling to 0.070", (5) vacuum annealing at 710°C for 30 min and furnace cooling, (6) diamond polishing the two parallel surfaces, and (7) rolling in one direction to an approximate thickness of 0.020", or a reduction of 70% (0.005" per pass).

### c. Aluminum alloy 7039\*

Cold-rolled with a (111) texture of 9R.

## PHASE EFFECT

If  $d_{\max}$ , or  $2\theta_{\min}$ , and  $f(0,\psi)$  or  $h$  (peak height) is measured from the (211) CrK $\alpha$  diffraction peak; ideally, from the Equations (1) and (2) the  $h_{\max}$  or  $f_{\max}$  should align with the  $2\theta_{\min}$ , as a function of  $\psi_0$  or  $\psi$ .

Such a plot, as shown in Figure 2, employing specimen 1, shows that such is not the case. A similar experiment conducted with cold-rolled Fe (specimen CR1) reveals a similar relationship in Figure 3. With such a mismatch in  $2\theta_{\min}$  and  $h_{\max}$  (the lag in  $2\theta_{\min}$  vs.  $\psi$  is defined as  $2\theta_L$ ) a large error in the computed residual stress can result. This error, however, is reduced as the stress increases.<sup>5</sup>

One of the objectives of the treatment that follows is to try to experimentally determine the factors governing this phase difference. It is hoped that even though these factors are found to be independent of such a phenomenon, that, at least they may be justifiably removed whenever an analysis of such an effect is considered.

## SYSTEMATIC ERRORS

The following parameters were tested and found to have a negligible effect on reducing the value of  $2\theta_L$ .

---

\*This specimen was fabricated and kindly furnished by A. Zarkades of AMMRC.

to note that this case represents the only condition, for the (211) reflection, where  $2\theta_{\min}$  and  $h_{\max}$  are aligned.

This particular experiment seems to support the suggestion that this  $2\theta_L$  effect is not necessarily due to large machining stress gradients.

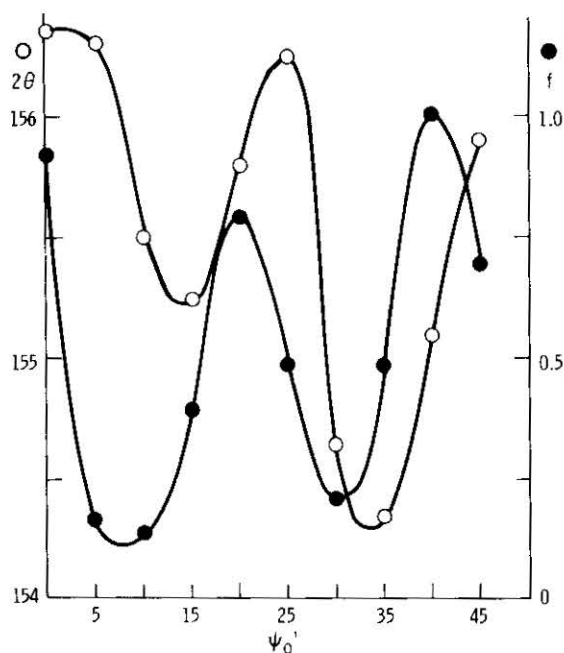


Figure 4.  $2\theta$  and  $h$  [CrK $\alpha$  (211)] vs.  $\psi_0'$ , for steel specimen 1, with scanning speed  $2\theta$  reduced to  $1^\circ/\text{min}$ .

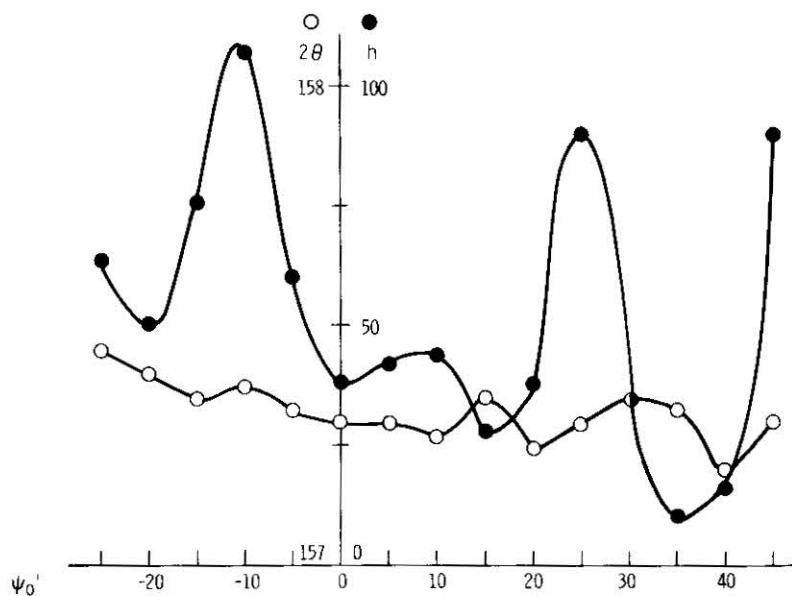


Figure 5.  $2\theta$  and  $h$  vs.  $\psi_0'$  for iron specimen CR1 after electropolishing the specimen surface.

a. Alignment of X-ray system

1. Receiving slit position

The procedure to test the effect of a variation in the alignment of receiving slit was to rotate the receiving slit until the  $2\theta$  peak position of standard specimens (i.e., Fe, Au, Al) were fixed at three distinct levels and subsequently repeating the  $2\theta$  and  $h$  vs.  $\psi$  experiment.

2. Specimen distance

The diffractometer was raised and lowered 2 mm in the direction of the specimen normal.

3. Specimen rotation along  $\psi_0$

To check on this effect, specimen 1 was rotated from the direction  $N_R$  (see Figure 1) by the displacement angle  $\delta$ .

b. Scanning rate and time constant

Specimen 1 was examined using a decreased scanning rate, i.e.,  $2\dot{\theta}=1^\circ/\text{min}$  (see Figure 4).

c. Variation in  $\phi$  of  $180^\circ$  (with and opposite R.D.)

d. Absorption

1. Random samples of steel (exhibiting less than 5% variation of  $x_R$  over an entire pole figure) and Al, were examined for loss of intensity with increasing  $\psi$ . The results are in agreement with theoretical calculations. This intensity correction was applied to the  $f(\alpha, \beta)$  distribution function.

2. The effect of the change in shape of the diffracted peak due to absorption and to the Lorentz Polarization factor on  $2\theta_L$  was also tested.

e. Grain size

To mitigate against the effect of grain size, the entire Rigaku goniometer is oscillated up to  $\pm 7^\circ$  in  $\psi$ , the time constant increased to 10 sec, and the scanning rate decreased to  $1^\circ/\text{min}$ . The grain size and distributions were determined metallographically and found to be elongated and large, varying from 10 to 80  $\mu\text{m}$  wide to 100 to 400  $\mu\text{m}$  long.

f. Polishing procedure

All specimens, such as 1, were mechanically polished using a procedure that was found to introduce no effect due to cold work. However, specimen CR1 was not mechanically polished.

Electropolishing specimen CR1 (see Figure 5) gave essentially the same results as the as-rolled condition shown in Figure 3. The only difference is the better resolution of the (111)  $[2\bar{1}\bar{1}]$   $2\theta_{\min}$  peak with electropolishing. It is interesting

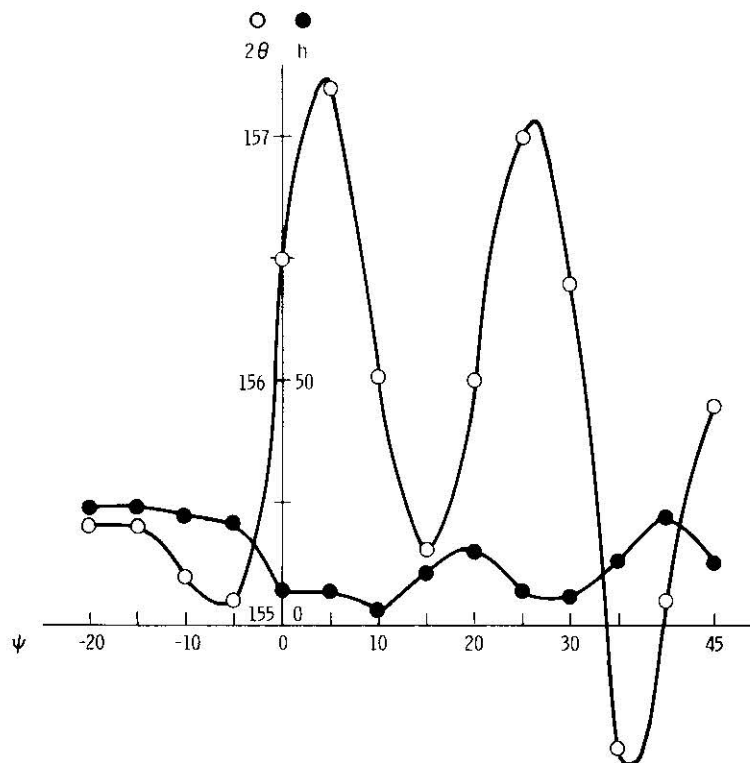


Figure 7.  $2\theta$  and  $h$  vs.  $\psi$  for steel specimen 1 with Rigaku divergent beam X-ray system ( $1^\circ$  receiving slit).

## REPRODUCIBILITY AND CONFIDENCE

The question of the reproducibility of the results presented in this report should be addressed.

Certainly more could have been done to isolate the characteristic textures. The main emphasis on reproducing data has been with the systematic errors of one parallel beam system. Supporting data was obtained with a divergent beam (Diano) and a quasi-divergent beam (Rigaku) system.

A decision was made to test specimens 1 and CRI on a similar parallel beam X-ray system in another laboratory. Experiments were repeated on a Rigaku Strainflex system at the Bethlehem Steel Co., Homer Research Laboratory. The results are shown in Figure 8. Compare the  $2\theta_L$  values of specimen 1 of approximately  $5^\circ$ ,  $8^\circ$ , and  $9^\circ$  (Figure 8) with the values of  $4^\circ$ ,  $5^\circ$ , and  $5^\circ$  reported in Figure 2.

## ALUMINUM TEXTURED ALLOY

As indicated by Dölle and Cohen, the  $\{hhh\}$  and the  $\{h00\}$  planes should not display any oscillation in the diffracted peak positions due to texture. The textured aluminum alloy was investigated under similar experimental conditions as those for steel using parallel beam optics; in fact the texture effect is absent, as the results given in Figures 9 and 10 show for the  $\{222\}$  planes. It may be seen that small oscillations occur both in the R.D. case and for the specimen rotated  $90^\circ$  to the R.D. This may be due to the large "effective" grain size. This problem was

## DIVERGENT BEAM GEOMETRY

A General Electric/Diano XRD-5 diffractometer afforded a divergent X-ray beam with Bragg Brentano focussing.

Specimen 1 was subjected to three levels of X-ray beam divergence. Although the condition affording the highest degree of divergence also provided the smallest "effective" particle size, (i.e.,  $1^\circ$  beam,  $0.1^\circ$  receiving slit), sufficient resolution was not achieved to measure  $2\theta_L$  until the vertical divergence of the beam was reduced with lead masks so that a  $0.100''$  high beam was allowed to pass thru the  $0.4^\circ$  beam slit. Since the X-ray intensity was so severely reduced under these conditions, the results show (see Figure 6) a very large scatter in the  $2\theta$  curve. In spite of this problem, a lag in  $2\theta_L$  remains at approximately  $5^\circ$ .

Finally, specimen 1 was examined on a Rigaku divergent beam diffractometer with a fixed specimen ( $\omega=0$ ) and a large receiving slit ( $1^\circ$ ). Figure 7 gives the same behavior as that using parallel beam optics,  $2\theta_L \approx 4-5^\circ$ .

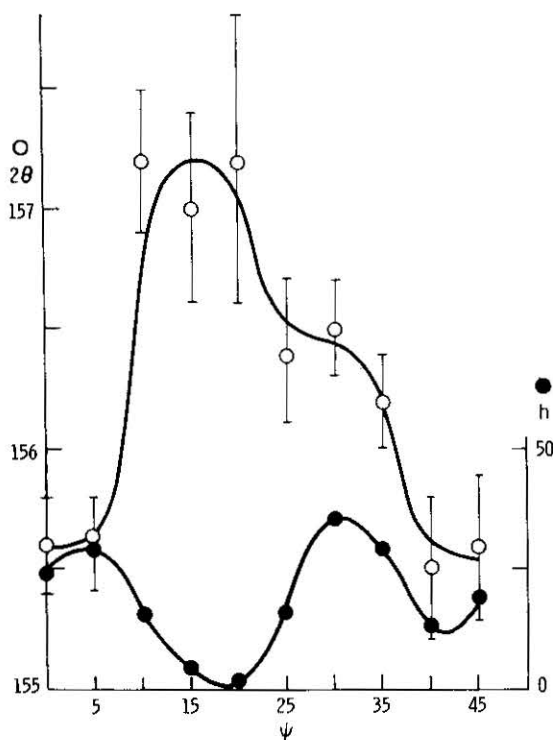


Figure 6.  $2\theta$  and  $h$  vs.  $\psi$  for steel specimen 1 with  $0.4^\circ$  beam slit and limited vertical divergence on the Diano system.

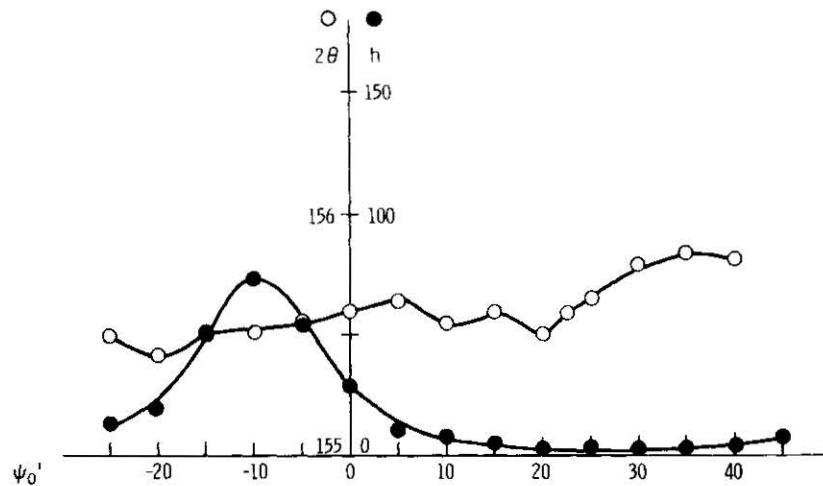


Figure 10.  $2\theta$  and  $h$  vs.  $\psi_0'$  for aluminum textured alloy specimen ( $\psi_0'$  in cross rolling direction).

observed earlier in an investigation of aluminum plate selected as standards for establishing a procedure for measuring residual stresses in aluminum.<sup>8</sup> In some cases, this problem of grain size was so severe that oscillations of  $\pm 7^\circ$  in  $\psi$  were necessary to eliminate the effect.

### CONCLUSIONS

The mismatch or lag in  $2\theta_{\min}$  (or  $d_{\max}$ ) behind the (211)  $K\alpha$  intensity maximum appears to be a real effect to contend with at least in the application of the Marion-Cohen method of correcting for texture in the application of parallel beam optics. Whether this behavior is due to microstrains, inhomogeneities, plastic anisotropy, large grain size, grain coupling, or other untested factors, they are present in the two forms of steel textures revealed in the results of this work.

Jaensson<sup>9</sup> has presented a provocative study of the effects of a fixed  $\psi$  angle system on the  $2\theta$  peak position. Although this factor should be given serious consideration for conducting texture corrections, the doublet separation in this study is approximately one degree  $2\theta$ , apparently not accounting for the full phase effect.

Although further experimental work is certainly in order to identify the origins of this effect, some recommendations can be made to reduce or correct for this  $2\theta_L$  effect.

Following the suggestion of Jaensson<sup>9</sup>, a  $\psi$ - $2\theta$  coupled goniometer may reduce  $2\theta_L$ . Along these lines, R. Chrenko, G.E. R&D Laboratory, Schenectady, N.Y., recently suggested that the side slope method employed with the  $\psi$  constant Rigaku Strainflex goniometer should be tested to effectively give the same conditions as suggested by Jaensson.

8. HORNUNG, N.L. X-Ray Stress Analysis Development of Aluminum Standards, Special AMMRC Report, in process.

9. JAENSSON, B. A Principal Distinction Between Different Kinds of X-Ray Equipment for Residual Stress Measurement, *Mat. Sci. and Engrg.*, v. 43, 1980, p. 169.

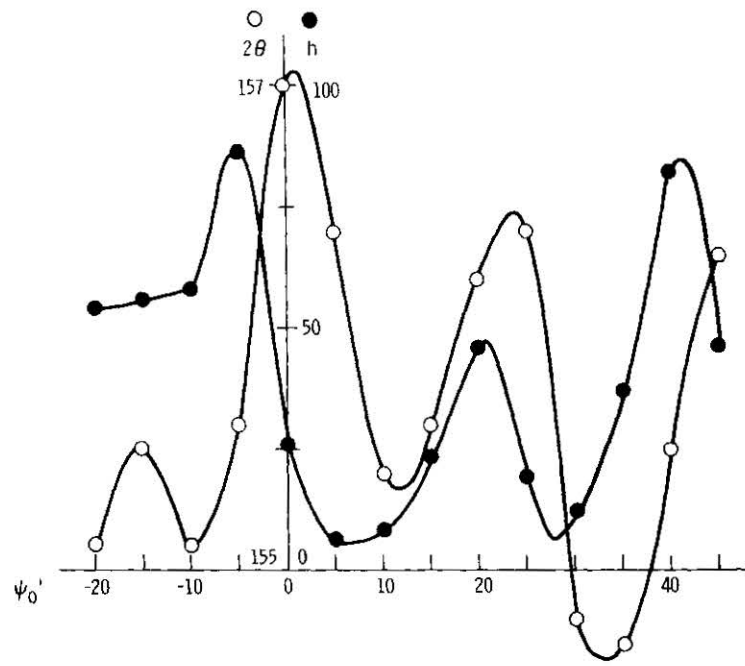


Figure 8.  $2\theta$  and  $h$  vs.  $\psi_0'$  for steel specimen 1 with Rigaku strainflex (at Homer Research Laboratory, Bethlehem Steel).

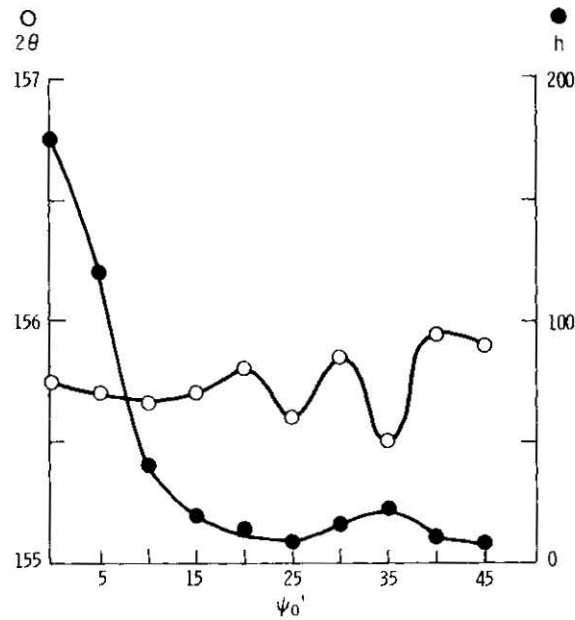


Figure 9.  $2\theta$  and  $h$   $[\text{CrK}\alpha (222)]$  vs.  $\psi_0'$  for aluminum textured alloy specimen ( $\psi_0'$  in rolling direction).



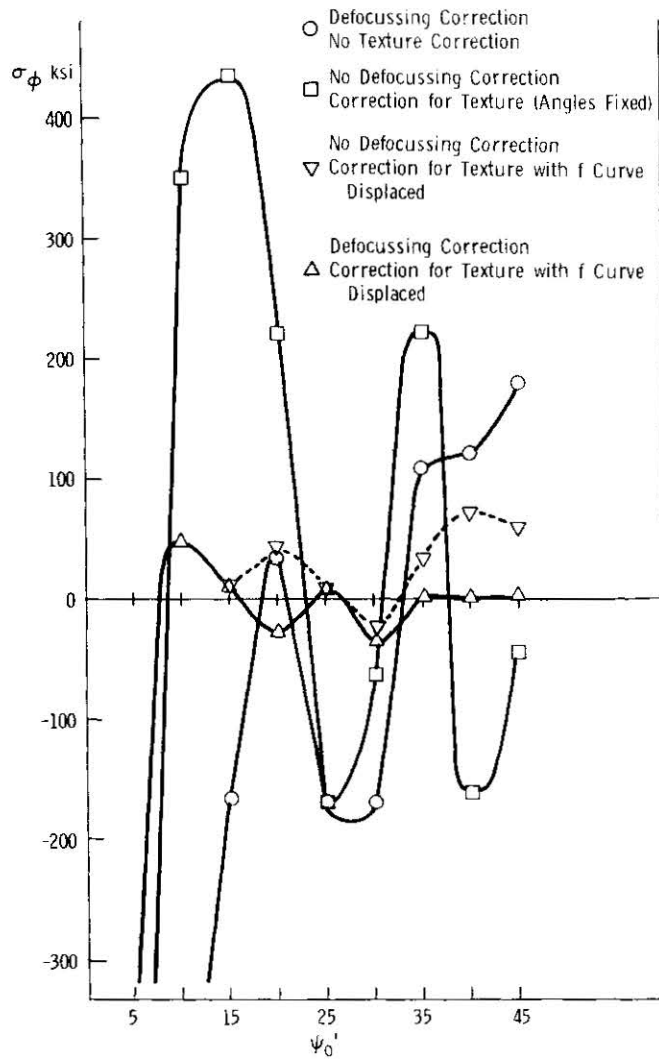


Figure 11. Measured residual stress  $\sigma_{\phi}$  vs.  $\psi'_0$  for steel specimen 1 showing effect of defocussing correction and setting  $2\theta_L = 0$  (displacing f curve).

#### ACKNOWLEDGMENTS

Thanks are extended to technicians T. Sheridan and F. Rudy for operating the X-ray equipment, to Prof. T. Ericsson for calling attention to Reference 9, to R. Chrenko of G.E. Research Lab. for his suggestions, to J. Chilton of Bethlehem Steel Co. for the data shown in Figure 8, to Rigaku/USA for the data illustrated in Figure 7, to Dr. J. B. Cohen for helpful reference referrals, to A. Zarkades for supplying the steel and aluminum textured samples, and to Dr. G. Bruggeman for his assistance in editing this paper.

1. The reduction of the average grain size by the use of a large divergent beam may be a means to reduce the  $2\theta_L$ . Jaensson suggests oscillating the goniometer to achieve the same result. It should be pointed out, however, that when this procedure is followed, the time constant of the detection system must be increased substantially.

2. Another method of increasing the number of grains is to increase the X-ray energy, thus permitting greater penetration of the X-rays into the steel.

3. Displace the  $f$  curve, matching  $2\theta_{\min}$  and the  $(211) K_{\alpha}$  maximum as demonstrated in Figure 11. This would reduce the error with the Marion-Cohen texture correction in determining the residual stress.

The suggestion of Dölle and Cohen<sup>2</sup> to employ  $\{hhh\}$  or  $\{h00\}$  reflections is of course available with the selection of the  $CuK_{\alpha}^*$  (400) steel reflection. However, another technique may be to use a non-dispersive technique (whereby the energy of the radiation is varied in the back reflecting region): add the shifts in  $\lambda$  or  $2\theta$  for several  $\{hkl\}$ s to "average out" the texture in the sample thereby avoiding a Marion-Cohen correction. This technique would increase the accuracy over the selection of the  $CrK_{\alpha}$  (200) steel reflection. [Presently, the  $CrK_{\alpha}$  (211) affords  $3\frac{1}{2}$  times the accuracy <sup>$\alpha$</sup>  over the  $CrK_{\alpha}$  (200) reflection.]

Another approach would be to use the  $CoK_{\alpha}$  (310) reflection to avoid the scattering vector from approaching the high concentrations of the  $\{310\}$  poles due to texture.<sup>1</sup> However, this technique demands further experimental work, due to the departure of practical textures from the ideal case, as well as other potential problems.

---

\*The use of the  $CuK_{\beta}$  radiation places some additional experimental restrictions on resolution of the (400) diffraction peak due to the fluorescence of the iron atoms. Although a monochromator increases the resolution, the price is a loss in X-ray intensity.

# DISTRIBUTION LIST

No. of Copies	To	No. of Copies	To
1	Office of the Under Secretary of Defense for Research and Engineering, The Pentagon, Washington, DC 20301	1	President, Airborne, Electronics and Special Warfare Board, Fort Bragg, NC 28307 ATTN: Library
12	Commander, Defense Technical Information Center, Cameron Station, Building 5, 5010 Duke Street, Alexandria, VA 22314	1	Director, U.S. Army Ballistic Research Laboratory, Aberdeen Proving Ground, MD 21005 ATTN: DRDAR-TSB-S (STINFO)
1	Battelle Columbus Laboratories, Metals and Ceramics Information Center, 505 King Avenue, Columbus, OH 43201	1	Commander, Dugway Proving Ground, Dugway, UT 84022 ATTN: Technical Library, Technical Information Division
1	Deputy Chief of Staff for Research, Development, and Acquisition, Headquarters, Department of the Army, Washington, DC 20301 ATTN: DAMA-ARZ	1	Commander, Harry Diamond Laboratories, 2800 Powder Mill Road, Adelphi, MD 20783 ATTN: Technical Information Office
1	Commander, Army Research Office, P.O. Box 12211, Research Triangle Park, NC 27709 ATTN: Information Processing Office	1	Chief, Benet Weapons Laboratory, LCWSL, USA ARRADCOM, Watervliet, NY 12189 ATTN: DRDAR-LCB-TL
1	Commander, U.S. Army Materiel Development and Readiness Command, 5001 Eisenhower Avenue, Alexandria, VA 22333 ATTN: DRCLDC	1	Dr. T. Davidson
1	Commander, U.S. Army Materiel Systems Analysis Activity, Aberdeen Proving Ground, MD 21005 ATTN: DRXSY-MP, H. Cohen	1	Mr. D. P. Kendall
1	Commander, U.S. Army Electronics Research and Development Command, Fort Monmouth, NJ 07703 ATTN: DELSD-L	1	Commander, U.S. Army Foreign Science and Technology Center, 220 7th Street, N. E., Charlottesville, VA 22901 ATTN: Military Tech, Mr. Marley
1	DELS-D	1	Commander, U.S. Army Aeromedical Research Unit, P.O. Box 577, Fort Rucker, AL 36360 ATTN: Technical Library
1	Commander, U.S. Army Missile Command, Redstone Arsenal, AL 35809 ATTN: DRSMI-RKP, J. Wright, Bldg. 7574	1	Director, Eustis Directorate, U.S. Army Air Mobility Research and Development Laboratory, Fort Eustis, VA 23604 ATTN: Mr. J. Robinson, DAVDL-E-MOS (AVRADCOM)
4	DRSMI-TB, Redstone Scientific Information Center	1	U.S. Army Aviation Training Library, Fort Rucker, AL 36360 ATTN: Building 5906-5907
1	DRSMI-RLM	1	Commander, U.S. Army Agency for Aviation Safety, Fort Rucker, AL 36362 ATTN: Technical Library
1	Technical Library	1	Commander, USACDC Air Defense Agency, Fort Bliss, TX 79916 ATTN: Technical Library
2	Commander, U.S. Army Armament Research and Development Command, Dover, NJ 07801 ATTN: Technical Library	1	Commander, U.S. Army Engineer School, Fort Belvoir, VA 22060 ATTN: Library
1	DRDAR-SCM, J. D. Corrie	1	Commander, U.S. Army Engineer Waterways Experiment Station, Vicksburg, MS 39180 ATTN: Research Center Library
1	DRDAR-QAC-E	1	Commander, U.S. Army Environmental Hygiene Agency, Edgewood Arsenal, MD 21010 ATTN: Chief, Library Branch
1	DRDAR-LCA, Mr. Harry E. Peibly, Jr., PLASTEC, Director	1	Technical Director, Human Engineering Laboratories, Aberdeen Proving Ground, MD 21005 ATTN: Technical Reports Office
1	Commander, U.S. Army Natick Research and Development Laboratories, Natick, MA 01760 ATTN: Technical Library		
1	Commander, U.S. Army Satellite Communications Agency, Fort Monmouth, NJ 07703 ATTN: Technical Document Center		
1	Commander, U.S. Army Tank-Automotive Command, Warren, MI 48090 ATTN: DRSTA-RKA		
2	DRSTA-UL, Technical Library		
1	Commander, White Sands Missile Range, NM 88002 ATTN: STEWS-WS-VT		

## REFERENCES

1. DÖLLE, H. The Influence of Multiaxial Stress States, Stress Gradients and Elastic Anisotropy on the Evaluation of Residual Stresses by X-Rays, J. Appl. Cryst, v. 12, 1979, p. 489.
2. DÖLLE, H., and COHEN, J. B. Evaluation of Residual Stresses in Textured Cubic Metals, Met. Trans. A., v. 11A, 1980, p. 831.
3. MARION, R. H., and COHEN, J. C. Anomalies in Measurement of Residual Stress by X-Ray Diffraction, Adv. X-Ray Anal., v. 18, 1975, p. 466.
4. WEIDEMANN, W. Phd. Thesis, Technische Hochschule, Aachen, Germany, 1966, Synopsis in Bollenroth, V. F., and Hauk, V. Zur Dentung der Gittereigenverformungen in plastisch verformtem-Eisen, Arch fur Eisen, v. 10, 1967, p. 793.
5. SHIRAIWA, T., and SAKAMOTO, Y. The X-Ray Stress Measurement of the Deformed Steel Having Preferred Orientation, Soc. Mat. Sci., 1970, Kyoto, Japan, p. 25.
6. DOLLE, H., and HAUK, V. Einfluss der Mechanischen Anisotropie de Vielkristalls (Textur) auf die Rontgenogriphische Spannungermittlung, v. 69, 1978, p. 410.
7. HAUK, V., and SESEMANN, H. Abweichungen von Linearen Gitterbenenabstandsverteilungen in Kubischen Metallen und ihre Berucksichtigung bei der Rontgenographischen Spannungermittlung, v. 67, 1976, p. 646.
8. HORNUNG, N. L. X-Ray Stress Analysis Development of Aluminum Standards, Special AMMRC Report, in process.
9. JAENSSON, B. A Principal Distinction Between Different Kinds of X-Ray Equipment for Residual Stress Measurement, Mat. Sci. and Engrg., v. 43, 1980, p. 169.

No. of Copies	To
1	Commandant, U.S. Army Quartermaster School, Fort Lee, VA 23801 ATTN: Quartermaster School Library
1	Commander, U.S. Army Radio Propagation Agency, Fort Bragg, NC 28307 ATTN: SCCR-2
1	Naval Research Laboratory, Washington, DC 20375 ATTN: Dr. J. M. Krafft - Code 5830
2	Dr. G. R. Yoder - Code 6384
1	Chief of Naval Research, Arlington, VA 22217 ATTN: Code 471
2	Commander, U.S. Air Force Wright Aeronautical Laboratories, Wright-Patterson Air Force Base, OH 45433 ATTN: AFWAL/MLSE, E. Morrissey
1	AFWAL/MLC
1	AFWAL/MLLP, M. Forney Jr.
1	AFWAL/MLBC, Mr. Stanley Schulman
1	National Aeronautics and Space Administration, Washington, DC 20546 ATTN: Mr. B. G. Achhammer
1	Mr. G. C. Deutsch - Code RW
1	National Aeronautics and Space Administration, Marshall Space Flight Center, Huntsville, AL 35812 ATTN: R. J. Schwinghammer, EH01, Dir, M&P Lab
1	Mr. W. A. Wilson, EH41, Bldg. 4612
1	Ship Research Committee, Maritime Transportation Research Board, National Research Council, 2101 Constitution Ave., N. W., Washington, DC 20418

No. of Copies	To
1	Librarian, Materials Sciences Corporation, Blue Bell Campus, Merion Towle House, Blue Bell, PA 19422
1	Panametrics, 221 Crescent Street, Waltham, MA 02154 ATTN: Mr. K. A. Fowler
1	The Charles Stark Draper Laboratory, 68 Albany Street, Cambridge, MA 02139
1	Lockheed-Georgia Company, 86 South Cobb Drive, Marietta, GA 30063 ATTN: Materials and Processes Engineering Dept. 71-11, Zone 54
1	General Dynamics, Convair Aerospace Division, P.O. Box 748, Fort Worth, TX 76101 ATTN: Mfg. Engineering Technical Library
1	Mechanical Properties Data Center, Belfour Stulen Inc., 13917 W. Bay Shore Drive, Traverse City, MI 49684
1	Dr. Robert S. Shane, Shane Associates, Inc., 7821 Carrleigh Parkway, Springfield, VA 22152
1	Mr. R. J. Zentner, EAI Corporation, 198 Thomas Johnson Drive, Suite 16, Frederick, MD 21701
2	Director, Army Materials and Mechanics Research Center, Watertown, MA 02172 ATTN: DRXMR-PL
1	Author